Theoret. chim. Acta (Berl.) 9, 151—170 (1967)

Magnetic Properties of Transition Metal Ion Cubic $^5T_2$ Terms in Axial Ligand Fields

I. Magnetic Anisotropy and Principal Magnetic Susceptibilities

E. KÖNIG* and A. S. CHAKRAVARTY**

Mellon Institute, Pittsburgh, Pennsylvania 15213, USA

Received August 28, 1967

The theory of magnetic anisotropy and susceptibility is worked out for cubic $^5T_2$ terms, the degeneracy of which is partially lifted by a ligand field component of axial symmetry as well as by spin-orbit coupling. Matrix elements are calculated by application of the method of ABRAGAM and PRYCE to a set of M.O. based wave-functions. The anisotropy in covalency of the metal-ligand bond and in spin-orbit coupling is taken into account. Numerical values of principal magnetic moments, $P_\parallel$ and $P_\perp$, are calculated as function of kT/λ, δ/λ, and $\varkappa$.

The theoretical results are employed in a rigorius analysis of existing single crystal magnetic data on high-spin iron(II) compounds. For $(NH_4)_2Fe(SO_4)_2 \cdot 6\,H_2O$, $\lambda = -100\ cm^{-1}$, $\delta = 1070\ cm^{-1}$ and $\varkappa = 0.8$ to 0.6 is obtained. For $FeSiF_6 \cdot 6\,H_2O$, $\lambda = -80\ cm^{-1}$, $\delta = -760\ cm^{-1}$ at 77.3 °K and $-580\ cm^{-1}$ between 20.4 and 1.57 °K, and $\varkappa \sim 0.7$ is derived. No unique fit is possible for $K_2Fe(SO_4)_2 \cdot 6\,H_2O$. The data are reproduced to better than $\pm 1\%$ in most cases. The limitations of the approach are stressed.

Die Theorie der magnetischen Anisotropie und der magnetischen Suszeptibilität eines $^5T_2$ Grundterms im oktaedrischen Ligandenfeld wird für den Fall entwickelt, daß die Entartung unter dem Einfluß einer axial-symmetrischen Feldkomponente sowie der Spin-Bahn-Wechselwirkung teilweise aufgehoben ist. Eigenfunktionen werden auf der Grundlage der M.O.-Theorie aufgestellt, Matrixelemente mittels der Theorie von ABRAGAM und PRYCE ermittelt. Der Anisotropie der Metall-Ligand-Bindung sowie der Spin-Bahn-Kopplung wird Rechnung getragen. Numerische Werte für die magnetischen Hauptmomente $P_\parallel$ und $P_\perp$ werden in Abhängigkeit von kT/λ, δ/λ und $\varkappa$ berechnet.

Die Ergebnisse der Theorie werden für eine genaue Analyse der verfügbaren magnetischen Daten aus Messungen an Einkristallen magnetisch normaler Eisen(II)-Verbindungen verwendet. Für $(NH_4)_2Fe(SO_4)_2 \cdot 6\,H_2O$ werden $\lambda = -100\ cm^{-1}$, $\delta = 1070\ cm^{-1}$ und $\varkappa = 0{,}8$ bis 0,6 erhalten. Für $FeSiF_6 \cdot 6\,H_2O$ ergeben sich $\lambda = -80\ cm^{-1}$, $\delta = -760\ cm^{-1}$ bei 77,3 °K und $\delta = -580\ cm^{-1}$ zwischen 20,4 und 1,57 °K sowie $\varkappa \sim 0{,}7$. Die experimentellen Daten können in den meisten Fällen auf $\pm 1\%$ genau oder besser wiedergegeben werden. Bei $K_2Fe(SO_4)_2 \cdot 6\,H_2O$ gelang keine eindeutige Bestimmung der theoretischen Parameter. Die Grenzen der vorliegenden Behandlung werden kritisch diskutiert.

La théorie de l'anisotropie magnétique et de la susceptibilité magnétique est développée pour les termes cubiques $^5T_2$, dont la dégénerescence est partiellement levée par une composante à symétrie axiale du champ de ligandes ainsi que par le couplage spin-orbite. Les éléments de matrice sont calculés à l'aide de la méthode d'ABRAGAM et PRYCE employée sur un système M.O. des fonctions d'onde de base. On a pris en consideration l'anisotropie de la liaison entre le metal et le ligand et aussi du couplage spin-orbite. Les valeurs numériques des moments magnétiques principaux $P_\parallel$ et $P_\perp$ sont calculées en fonction de kT/λ, δ/λ, et $\varkappa$.

* Visiting Fellow, Inorganic Chemistry, 1962—1965. Present adress: Institut für Physikalische Chemie, Universität Erlangen-Nürnberg, Germany.

** Postdoctoral Fellow, Theoretical Chemistry, 1963—1964. Present adress: Saha Institute of Nuclear Physics, Calcutta-9, India.

Les résultats théoriques sont employés dans une analyse détaillée des données magnétiques disponibles sur monocristaux des composés ferreux spin-élevés. Pour $(NH_4)_2Fe(SO_4)_2 \cdot 6\ H_2O$ on a obtenu $\lambda = -100\ cm^{-1}$, $\delta = 1070\ cm^{-1}$ et $\varkappa = 0.8$ à 0,6. Pour $FeSiF_6 \cdot 6\ H_2O$ on a eu comme résultat $\lambda = -80\ cm^{-1}$, $\delta = -760\ cm^{-1}$ à 77,3 °K et $\delta = -580\ cm^{-1}$ entre 20,4 et 1,57 °K avec $\varkappa \sim 0{,}7$. Les valeurs expérimentales sont réprésentées dans la plupart de cas plus précises que $\pm 1\%$. Au cas de $K_2Fe(SO_4)_2 . 6\ H_2O$ une détermination unique était impossible. Les limites de cette approximation sont discutées.

Introduction

The principal molecular susceptibilities of cubic ${}^5T_2$ terms with a tetragonal distortion superimposed, were calculated previously with respect to the specific example of iron(II) ammonium Tutton salt by BOSE et al. [1]. A trigonal field as a distortion of cubic symmetry has been treated in a different approach based on third order perturbation by the $\lambda \boldsymbol{L} \cdot \boldsymbol{S}$ term by PALUMBO [2] in order to explain the temperature dependence of the principal susceptibilities of iron(II) fluosilicate, $FeSiF_6 \cdot 6H_2O$. This treatment includes levels belonging to $M_J = 0$ and $M_J = \pm 1$ only. More recently, the susceptibility of the same compound was calculated in a limited range of temperature by EICHER [3]. In all these cases, a crystal field approach was employed.

However, a recalculation by the present authors has shown that reasonable agreement with experimental data for iron(II) Tutton salts cannot be achieved within this approximation. Therefore, the principal molecular susceptibilities $K_\parallel$ and $K_\perp$ of ${}^5T_2$ terms in axial fields are calculated at present using an approach based on molecular orbitals. The axial field is considered here to include field components of both tetragonal and trigonal symmetry. In addition, the treatment is extended by taking into account the anisotropy in covalency of the metal-ligand bond as well as in spin-orbit coupling. The numerical results are plotted for the applicable range of the parameters kT/λ, δ/λ and $\varkappa$, and a comparison with the available experimental data is presented.

Fine Structure Levels and Wave-Functions

In most high-spin compounds of iron(II) which were investigated by methods of structure analysis and, likewise, in those of cobalt(III), the microsymmetry about the central ion is essentially octahedral with some tetragonal or trigonal distortion*. The ligand field potential may thus be written as [9]

$$V = V_{\text{cubic}} + V_{\text{axial}} . \tag{1}$$

The predominant cubic field splits the atomic ${}^5D$ ground term into ${}^5T_2$ and the approximately 10,000 cm^{-1} higher-lying ${}^5E$. If the crystalline field axes are

* The X-ray structure of FeF_2 (tetragonal, space group D_{4h}^{14}) shows that the Fe^{2+} ion is surrounded by a distorted octahedron of six fluoride ions [4]. Octahedral coordination of Fe^{2+} ions is also involved in the CdI_2-type structure of $FeBr_2$ and FeI_2, hexagonal, D_{3d}^3, and the $CdCl_2$-type structure of $FeCl_2$, D_{3d}^5 [5]. In the monoclinic iron(II) Tutton salts, the coordination octahedron is tetragonally elongated [6]. In the rhombohedral $FeSiF_6 \cdot 6\ H_2O$, the distortion seems to be of trigonal symmetry [7]. X-ray structural studies have also shown octahedrally coordinated units to be present in $FeCl_2 \cdot 6\ H_2O$, $FeSO_4 \cdot 7\ H_2O$, $Fe(ClO_4)_2 \cdot 6\ H_2O$, and in the ion $[Fe(NH_3)_6]^{2+}$ [8]. Finally, octahedral coordination is well established in iron(II) porphyrins.

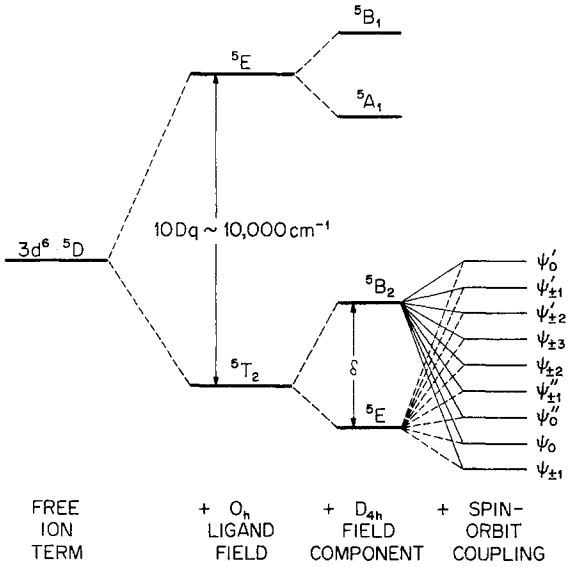

Fig. 1. Energy level diagram for a $^5D(d^6)$ term under the influence of a tetragonal field ($\delta > 0$) and of spin-orbit coupling (not to scale)

chosen to pass through the ligand ions, V_{axial} corresponds to tetragonal symmetry. The additional splitting of the $^5T_2$ term is into ^5E and $^5B_2$, the separation being called δ (viz. Fig. 1). If the distortion is of trigonal symmetry, the z axis is usually taken along the (1,1,1) direction of the octahedron, and the $^5T_2$ term is split into ^5E and $^5A_1$. Since it has been shown [10], that with distortions of both tetragonal and trigonal symmetry, either one of the resulting levels may be lowest, in what follows only the distinction between $\delta > 0$ and $\delta < 0$ will be made. The sign of δ will be chosen as positive, whenever the orbital doublet ^5E is lowest. Also, off-diagonal matrix elements of the trigonal potential between the low-lying and higher ^5E terms will be disregarded, thus limiting our discussion to $\delta \ll 10$ Dq.

An additional splitting is introduced by spin-orbit coupling. In general, the spin-orbit coupling constant λ_i used here will be different from that of the free ion, $\lambda_i^{\text{free}} = \pm \zeta_i/2S$, since we assume a departure of our actual orbits from pure d orbitals*. The only additional modification required by partly covalent bonding involves the operator of Zeeman energy. It has been shown [11, 12] that matrix elements of the operator $\boldsymbol{L}$ are related by

$$\langle \varphi_n \mid \boldsymbol{L} \mid \varphi_m \rangle = \varkappa_{nm} \langle d_n \mid \boldsymbol{L} \mid d_m \rangle , \tag{2}$$

if φ_n designates molecular orbitals, d_n the corresponding free-atom orbitals, and $\varkappa_{nm}$ the components of the tensor of orbital reduction [13]. The magnetic operator thus obtains as $\beta \boldsymbol{H}(\varkappa \boldsymbol{L} + 2\boldsymbol{S})$.

* The parametrization of λ_i has already been useful to rationalize the spectra of transition metal ions. Without making specific assumptions about details of the wave-functions, it seems to be impractical to relate matrix elements of $\lambda \boldsymbol{L} \cdot \boldsymbol{S}$ within a M.O. basis to those calculated for pure d orbitals [13].

The energies within the $^5T_2$ term may be calculated on the basis of ABRAGAM and PRYCE's theory [14] using the structural isomorphism between $^5T_2$ and ^5P. The matrix elements of the Hamiltonian*

$$\mathscr{H} = \delta(1 - L_z'^2) - \lambda_\parallel L_z' S_z - \lambda_\perp (L_x' S_x + L_y' S_y) \qquad (3)^{**}$$

have to be evaluated within the 15 states $| M_L M_S \rangle$ of a ^5P term classified according to their values of M_J. The matrices obtained by diagonalization of the 15×15 matrix for $\mathscr{H}$, the resulting energy expressions and wave-functions are listed in Appendix I.

The combined effect of an axial field and of spin-orbit interaction on a cubic $^5T_2$ term thus produces nine levels, namely three singlets and six doublets. In the case of $\delta > 0$, these levels are drawn in Fig. 1 in the order of increasing energy. If an axial field having $\delta < 0$ is operative, the order of levels will be changed. Particularly, φ_1 which is lowest for $\delta > 0$, will be replaced by φ_0, etc. Finally, the remaining degeneracy can be lifted by application of a magnetic field.

Principal Magnetic Susceptibilities

The energy E_n of any particular level of an atom or ion may be expressed as a power series in the applied magnetic field H

$$E_n = E_n^{(0)} + E_{nm}^{(1)} H + E_{nm}^{(2)} H^2 + \ldots, \qquad (4)$$

where $E_n^{(0)}$ is the energy of the unperturbed atom and $E_{nm}^{(1)}$ and $E_{nm}^{(2)}$ are the first- and second-order Zeeman energy terms, respectively. The latter two terms may be obtained by application of the magnetic operator**

$$\mathscr{H}_m = \beta \boldsymbol{H}(-\varkappa \boldsymbol{L}' + 2\boldsymbol{S}), \qquad (5)$$

resulting in

$$E_{nm}^{(1)} = \langle \psi_{nm} \mid \beta(-\varkappa \boldsymbol{L}' + 2\boldsymbol{S}) \mid \psi_{nm} \rangle \qquad (6)$$

and

$$E_{nm}^{(2)} = \sum_{n,m}{}' \frac{|\langle \psi_{nm} \mid \beta(-\varkappa \boldsymbol{L}' + 2\boldsymbol{S}) \mid \psi_{n'm'} \rangle|^2}{E_n - E_{n'}} . \qquad (7)$$

Finally, the magnetic susceptibility up to second order is determined by [15]

$$K = N \frac{\sum_{n,m} [(E_{nm}^{(1)})^2/kT - 2E_{nm}^{(2)}] e^{-E_n^{(0)}/kT}}{\sum_n e^{-E_n^{(0)}/kT}} , \qquad (8)$$

where N is the Avogadro number and k the Boltzmann constant. To obtain the principal susceptibilities for systems with axial symmetry, Eq. (8) has to be calculated both in the direction parallel and perpendicular to the principal axis separately. The appropriate magnetic operators may be written as

$$\mu_\parallel = \beta(-\varkappa_\parallel L_z' + 2S_z) \qquad (9)$$

and

$$\mu_\perp = \beta(-\tfrac{1}{2}\varkappa_\perp L_-' - \tfrac{1}{2}\varkappa_\perp L_+' + S_- + S_+) \qquad (10)$$

* If the basic d orbitals are augmented by a contribution from p orbitals of the ligands, the overlap between both charge clouds may be influenced by the asymmetry of the ligand field. Therefore, in general both λ_i and $\varkappa_i$ may be anisotropic.

** $-\boldsymbol{L}'$ denotes the operator obtained according to [14]; $-\boldsymbol{L}'$ is isomorphic to $\boldsymbol{L}$.

respectively, where $L_\pm = L_x \pm iL_y$, $S_\pm = S_x \pm iS_y$, and where $\varkappa_\parallel$ and $\varkappa_\perp$ are defined by Eq. (2) [16].

a) Axial Field, $\delta > 0$

Performing the outlined calculation up to second order, one obtains in the case $\delta > 0$ the expressions for the principal molecular susceptibilities given below.

$$K_\parallel = \frac{N\beta^2}{kZ}\left\{\frac{1}{T}\left[G_{1z}^{E_1} + G_{1z}^{E_1''}\exp(\Theta_3/kT) + G_{1z}^{E_2}\exp(\Theta_4/kT) + \right.\right.$$
$$+ G_{1z}^{E_3}\exp(\Theta_5/kT) + G_{1z}^{E_2'}\exp(\Theta_6/kT) + G_{1z}^{E_1'}\exp(\Theta_7/kT)] +$$
$$+ 2k[G_{2z}^{E_1} + G_{2z}^{E_0}\exp(\Theta_1/kT) + G_{2z}^{E_0''}\exp(\Theta_2/kT) + G_{2z}^{E_1''}\exp(\Theta_3/kT) +$$
$$+ G_{2z}^{E_2}\exp(\Theta_4/kT) + G_{2z}^{E_2'}\exp(\Theta_6/kT) + G_{2z}^{E_1'}\exp(\Theta_7/kT) +$$
$$\left.\left. + G_{2z}^{E_0'}\exp(\Theta_8/kT)]\right\}, \tag{11}$$

$$K_\perp = \frac{2N\beta^2}{Z}\left\{G_{2x}^{E_1} + G_{2x}^{E_0}\exp(\Theta_1/kT) + G_{2x}^{E_0''}\exp(\Theta_2/kT) + G_{2x}^{E_1''}\exp(\Theta_3/kT) + \right.$$
$$+ G_{2x}^{E_2}\exp(\Theta_4/kT) + G_{2x}^{E_3}\exp(\Theta_5/kT) + G_{2x}^{E_2'}\exp(\Theta_6/kT) +$$
$$\left. + G_{2x}^{E_1'}\exp(\Theta_7/kT) + G_{2x}^{E_0'}\exp(\Theta_8/kT)\right\}, \tag{12}$$

where

$$\begin{aligned} \Theta_1 &= E_1 - E_0\,, & \Theta_5 &= E_1 - E_3\,, \\ \Theta_2 &= E_1 - E_0''\,, & \Theta_6 &= E_1 - E_2'\,, \\ \Theta_3 &= E_1 - E_1''\,, & \Theta_7 &= E_1 - E_1'\,, \\ \Theta_4 &= E_1 - E_2\,, & \Theta_8 &= E_1 - E_0'\,, \end{aligned} \tag{13}$$

$$Z = 2 + \exp(\Theta_1/kT) + \exp(\Theta_2/kT) + 2\exp(\Theta_3/kT) + 2\exp(\Theta_4/kT) +$$
$$+ 2\exp(\Theta_5/kT) + 2\exp(\Theta_6/kT) + 2\exp(\Theta_7/kT) + \exp(\Theta_8/kT) \tag{14}$$

b) Axial Field, $\delta < 0$

In the case $\delta < 0$, the corresponding expressions for the principal molecular susceptibilities are

$$K_\parallel = \frac{N\beta^2}{kZ'}\left\{\frac{1}{T}\left[G_{1z}^{E_1}\exp(\Theta_1'/kT) + G_{1z}^{E_2}\exp(\Theta_2'/kT) + G_{1z}^{E_1'}\exp(\Theta_3'/kT) + \right.\right.$$
$$+ G_{1z}^{E_1''}\exp(\Theta_6'/kT) + G_{1z}^{E_2'}\exp(\Theta_7'/kT) + G_{1z}^{E_3}\exp(\Theta_8'/kT)] +$$
$$+ 2k\left[G_{2z}^{E_0} + G_{2z}^{E_1}\exp(\Theta_1'/kT) + G_{2z}^{E_2}\exp(\Theta_2'/kT) + G_{2z}^{E_1'}\exp(\Theta_3'/kT) + \right.$$
$$+ G_{2z}^{E_0''}\exp(\Theta_4'/kT) + G_{2z}^{E_0'}\exp(\Theta_5'/kT) + G_{2z}^{E_1''}\exp(\Theta_6'/kT) +$$
$$\left.\left. + G_{2z}^{E_2'}\exp(\Theta_7'/kT)]\right\}, \tag{15}$$

$$K_\perp = \frac{2N\beta^2}{Z'}G_{2x}^{E_0} + \left\{G_{2x}^{E_1}\exp(\Theta_1'/kT) + G_{2x}^{E_2}\exp(\Theta_2'/kT) + G_{2x}^{E_1'}\exp(\Theta_3'/kT) + \right.$$
$$+ G_{2x}^{E_0''}\exp(\Theta_4'/kT) + G_{2x}^{E_0'}\exp(\Theta_5'/kT) + G_{2x}^{E_1''}\exp(\Theta_6'/kT) +$$
$$\left. + G_{2x}^{E_2'}\exp(\Theta_7'/kT) + G_{2x}^{E_3}\exp(\Theta_8'/kT)\right\}, \tag{16}$$

where

$$\begin{aligned} \Theta_1' &= E_0 - E_1\,, & \Theta_5' &= E_0 - E_0'\,, \\ \Theta_2' &= E_0 - E_2\,, & \Theta_6' &= E_0 - E_1''\,, \\ \Theta_3' &= E_0 - E_1'\,, & \Theta_7' &= E_0 - E_2'\,, \\ \Theta_4' &= E_0 - E_0''\,, & \Theta_8' &= E_0 - E_3\,, \end{aligned} \tag{17}$$

$$Z' = 1 + 2\exp(\Theta_1'/kT) + 2\exp(\Theta_2'/kT) + 2\exp(\Theta_3'/kT) + \exp(\Theta_4'/kT) + \\ + \exp(\Theta_5'/kT) + 2\exp(\Theta_6'/kT) + 2\exp(\Theta_7'/kT) + 2\exp(\Theta_8'/kT)\,. \tag{18}$$

The matrix elements G_j and A_j are listed in Appendix II. All other matrix elements of $\mu_\parallel$ and $\mu_\perp$ are zero.

Results

The numerical results of our calculations are conveniently presented in terms of the principal magnetic moments $P_\parallel$ and $P_\perp$. The moments P_i, $i = \parallel$ or $\perp$, are related to $K_\parallel$ and $K_\perp$ by

$$P_i^2 = \frac{3k}{N\beta^2} K_i\, T\,, \tag{19}$$

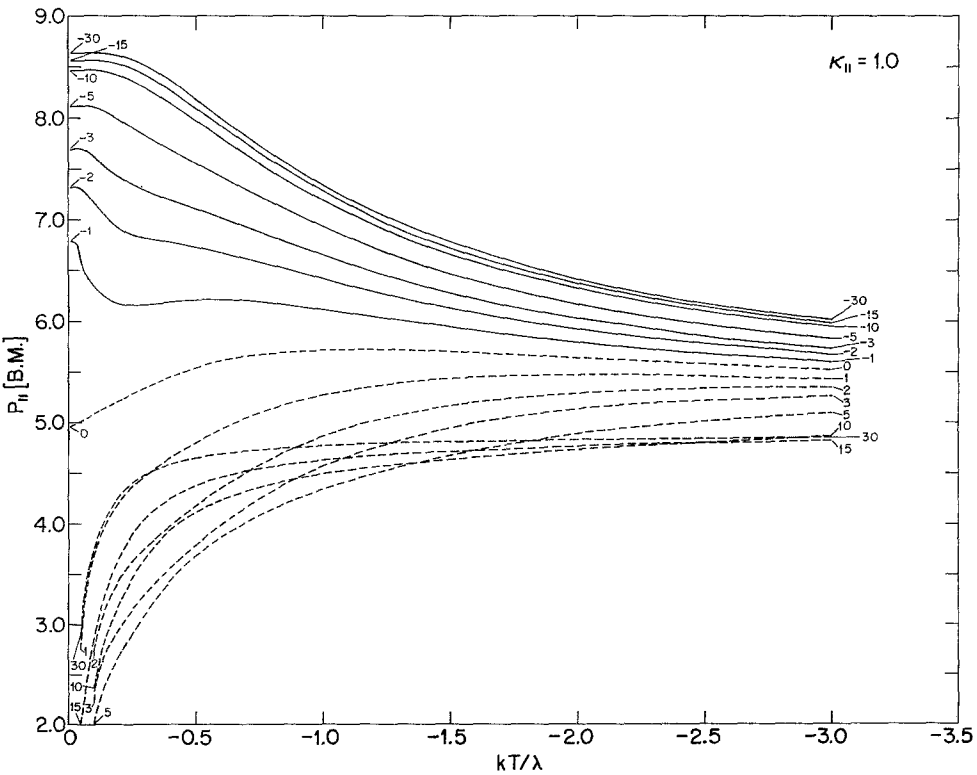

Fig. 2. Principal magnetic moment $P_\parallel$ (in B.M.) for a $^5T_2$ term under the influence of an axial ligand field and spin-orbit coupling. Values of δ/λ listed at end of each curve. Full curves for $\delta > 0$, broken curves for $\delta < 0$. $\varkappa_\parallel = 1.0$

where $K_\parallel$ and $K_\perp$ are expressed by Eq. (11) to (18). The moments are unique functions of the parameters kT/λ, δ/λ, and $\varkappa$, which are used within the following ranges of values:

$$\begin{aligned} kT/\lambda: &\quad -0.01 \text{ to } -5.0 \\ \delta/\lambda: &\quad 0 \text{ to } -30.0, \text{ if } \delta > 0 \\ &\quad 0 \text{ to } +30.0, \text{ if } \delta < 0 \\ \varkappa_\parallel \text{ and } \varkappa_\perp: &\quad 1.0 \text{ to } 0.5. \end{aligned}$$

The spin-orbit coupling constant λ has always been considered to have negative values, since these apply to the configuration $t_{2g}^4 e_g^2$. For convenience of presentation, we use in the following $\lambda_\parallel = \lambda_\perp = \lambda$. Representative examples of the results are illustrated in Fig. 2 to 5*. These plots are generally applicable to all d^6 high-spin systems in axially distorted octahedral symmetry, as long as the influence of co-operative effects remains negligible.

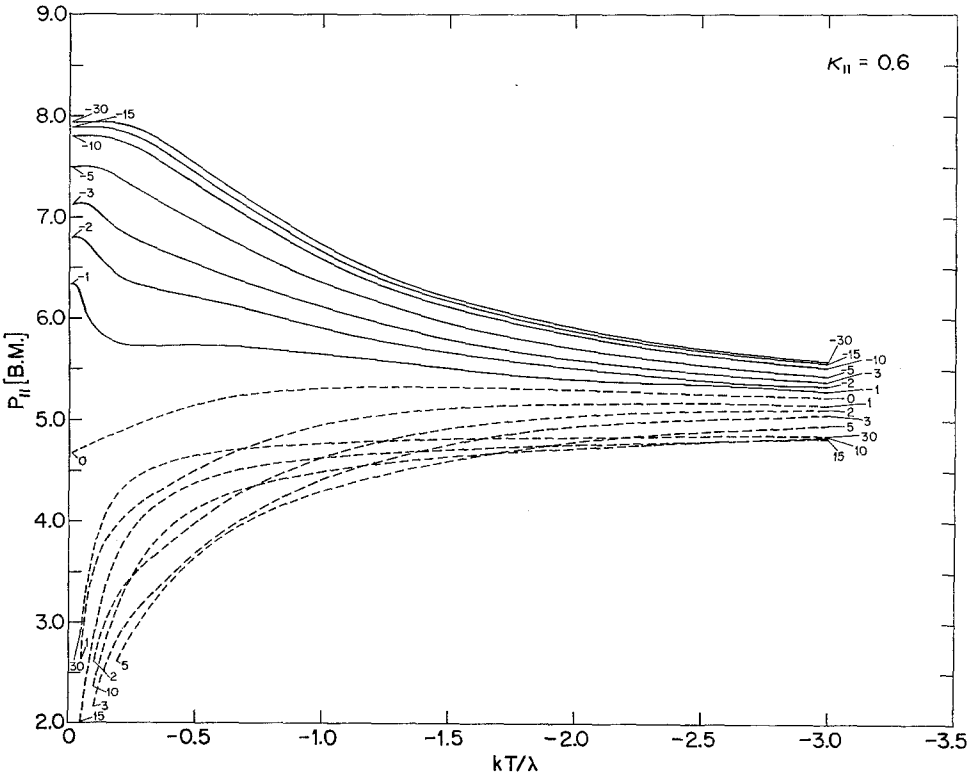

Fig. 3. Principal magnetic moment $P_\parallel$ (in B.M.) as in Fig. 2. $\varkappa_\parallel = 0.6$

Comparison with Experiment

Measurements of principal magnetic susceptibilities and/or magnetic anisotropies are available for several iron(II) Tutton salts [17—21], the corresponding iron(II) thallium selenate [19], $FeSO_4 \cdot 7\,H_2O$ [17, 20, 22], and $FeSiF_6 \cdot 6\,H_2O$

* Tables of numerical values for the principal magnetic moments $P_\parallel$ and $P_\perp$ may be obtained from the authors on request.

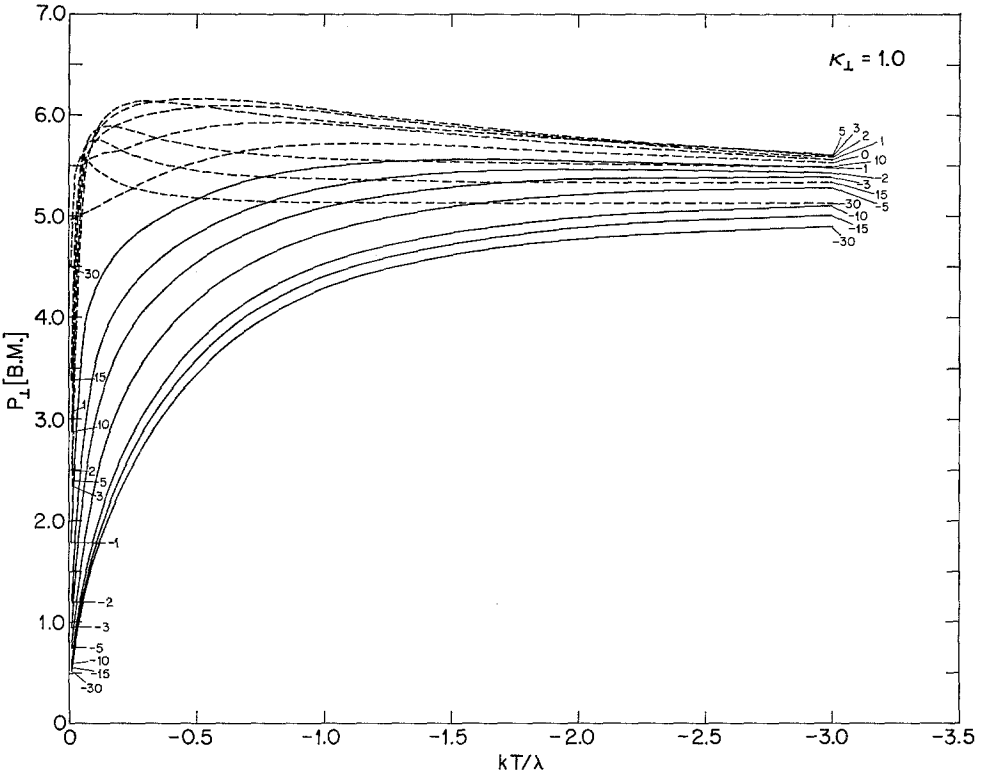

Fig. 4. Principal magnetic moment $P_\perp$ (in B.M.) as in Fig. 2. $\varkappa_\perp = 1.0$

[23, 24]. Suitable results for our purpose are, for example, those on iron(II) Tutton salts which are monoclinic with two molecules per unit cell. Since the octahedron of water molecules surrounding each Mg^{2+} ion in $(NH_4)_2Mg(SO_4)_2 \cdot 6\,H_2O$ is elongated along the z axis [6], and since all Tutton salts are isomorphous, it can safely be assumed that the symmetry around each Fe^{2+} ion is very nearly tetragonal. Denoting by α the angle between the z axis of the octahedron and the ac plane of the crystal, the principal crystal susceptibilities may be written as

$$\begin{aligned} \chi_1 &= K_\parallel \cos^2 \alpha + K_\perp \sin^2 \alpha \\ \chi_2 &= K_\perp \\ \chi_3 &= K_\parallel \sin^2 \alpha + K_\perp \cos^2 \alpha \,. \end{aligned} \tag{20}$$

Here, by convention, $\chi_1 > \chi_2$ and, since $\delta > 0$, $K_\parallel > K_\perp$. It follows that

$$\begin{aligned} K_\parallel - K_\perp &= 2\,(\chi_1 - \chi_2) - (\chi_1 - \chi_3) \\ K_\parallel &= (\chi_1 - \chi_2) + \chi_3 \\ K_\perp &= \chi_2 \,. \end{aligned} \tag{21}$$

These relations may be used to obtain the molecular susceptibilities $K_\parallel$ and $K_\perp$ and thus $P_\parallel$ and $P_\perp$ from the measured quantities χ_1, χ_2, and χ_3.

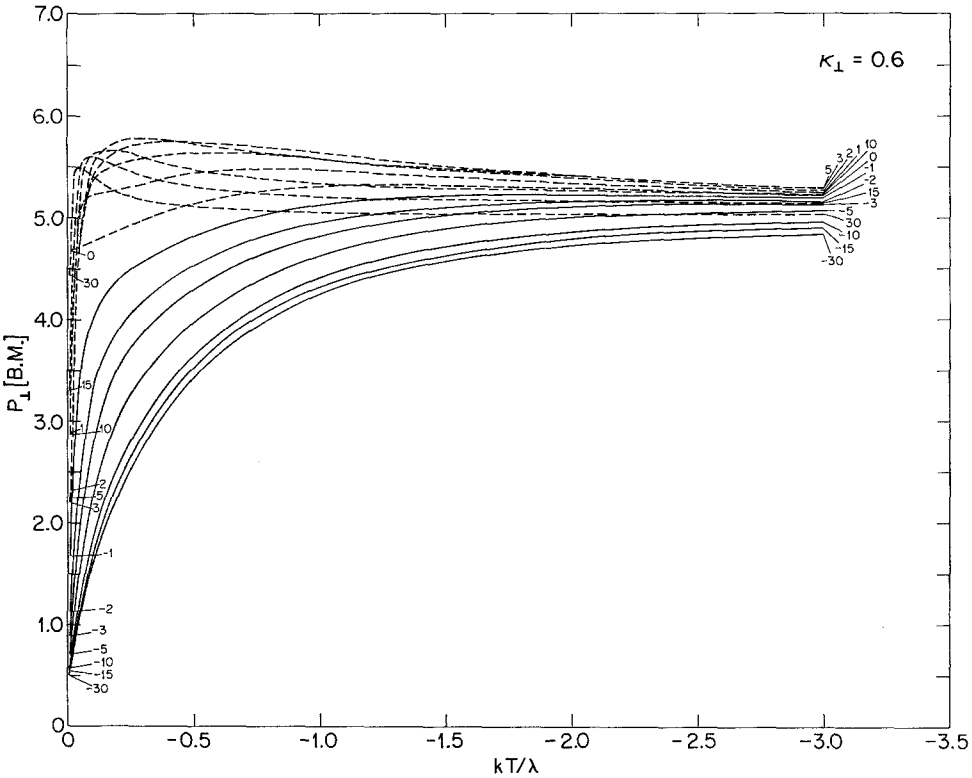

Fig. 5. Principal magnetic moment $P_\perp$ (in B.M.) as in Fig. 2. $\varkappa_\perp = 0.6$

Within the experimental results on iron(II) Tutton salts, we consider those of BOSE [21] as the most reliable ones. These data are therefore used for a comparison with the theory.*, **

It may be realized easily by inspection of Fig. 2 to 5 that, within the configuration d^6, a fitting of calculated principal moment curves to experimental data may not always be unambiguous. The following procedure is therefore adopted to obtain a reliable indication about the singularity of the fit. The sum of the squared deviations of calculated and experimental magnetic moments, viz.

$$\sum \Delta^2 = \Delta_\parallel^2 + 2\,\Delta_\perp^2\,, \tag{22}$$

where $\Delta_\parallel = P_\parallel^{\text{theor}} - P_\parallel^{\text{exp}}$, $\Delta_\perp = P_\perp^{\text{theor}} - P_\perp^{\text{exp}}$, is computed for each pair of values of the parameters δ/λ and $\varkappa$ (assuming $\varkappa_\parallel = \varkappa_\perp$). The results are mapped as

* We would like to point out an error which invalidates some of the conclusions of previous work. Inspection of the Table shows that the values for $P_\parallel$ and $P_\perp$ given by us differ considerably from those employed by BOSE et al. [1]. This is due to the fact that BOSE et al. used average values derived from Bose's experimental results [21] and those reported by JACKSON [25]. However, the values quoted by JACKSON apply in reality to $FeSO_4 \cdot 7\,H_2O$ (cf. [17]) rather than to the Tutton salt.

** In calculating $P_\parallel$ and $P_\perp$, $(3k/N\beta^2)^{1/2} = 2.8273$ was used. This value results if one employs the most recent values for the constants involved (cf. American Institute of Physics Handbook, McGraw-Hill, New York, 1963).

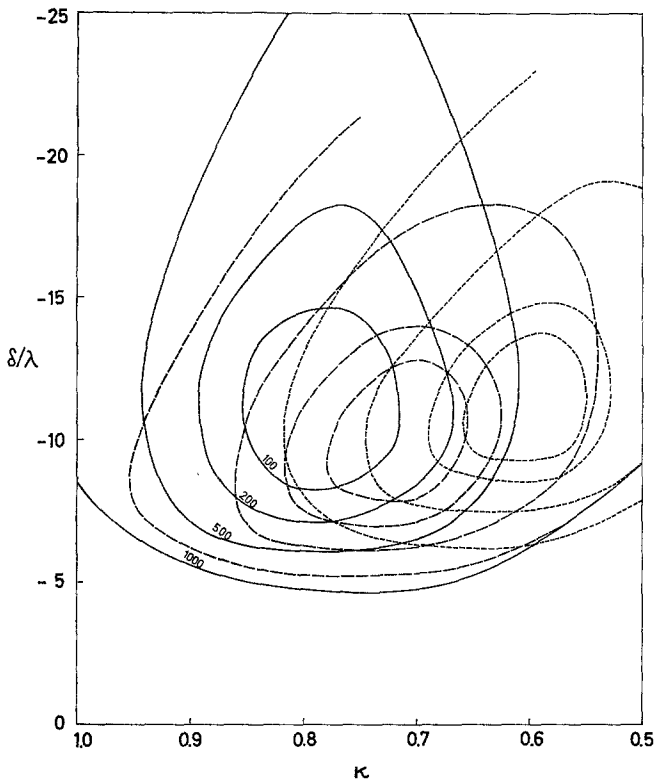

Fig. 6. Curves of constant $\Sigma\Delta^2$ for $(NH_4)_2Fe(SO_4)_2 \cdot 6\,H_2O$, assuming $\lambda = -100\ cm^{-1}$. Full curves for 296.8 °K, broken curves for 182.5 °K, dotted curves for 84.8 °K. Values of $\Sigma\Delta^2 \times 10^4$ are indicated on the curves

function of the afore-mentioned parameters at each available temperature and for an assumed value of λ. Curves of $\sum\Delta^2 = \text{const.}$ are then plotted and the plots repeated for modified λ values. If, for all the temperatures investigated, a minimum is clearly defined on the surface $\sum\Delta^2$, the corresponding values of λ, δ/λ, and $\varkappa$ are considered as providing the "best" fit. An example of such plots is shown in Fig. 6. However, if a "valley" is obtained rather than a minimum (cf. Fig. 7), or if the minimum is situated outside of the range of well-defined parameter values, this may occur for various reasons: (a) one or both of the experimental moment values, $P_\parallel$ and $P_\perp$, may be very inaccurate or seriously in error; (b) the theory may be inadaquate, e.g. due to large deviations from axial symmetry; (c) a change in the magnetic properties of the substance may take place due to co-operative phenomena, crystallographic phase transitions and alike. Under these circumstances, no general treatment is possible; rather each problem deserves individual consideration.

Turning our attention to the ammonium Tutton salt, $(NH_4)_2Fe(SO_4)_2 \cdot 6\,H_2O$, plots of $\sum\Delta^2 = \text{const.}$ are displayed in Fig. 6 for the three temperatures available. In these plots, practically the free ion value of λ, i.e. $\lambda = -100\ cm^{-1}$, was assumed. The resulting values of molecular parameters are listed in the Table. The best fit is described by almost constant values of $\delta/\lambda \sim -10$ and descreasing values of $\varkappa$ with

Table. *Comparison of experimental and calculated values for the principal magnetic moments*

Compound	Experimental Results					Theoretical Results (percentage deviation indicated in parentheses)				
	T °K	$K_\parallel$ 10^{-6} emu/mole	$K_\perp$	$P_\parallel$ B.M.	$P_\perp$ B.M.	$P_\parallel$ B.M.	$P_\perp$ B.M.	δ cm^{-1}	$\varkappa$	λ cm^{-1}
$(NH_4)_2Fe(SO_4)_2 \cdot 6\,H_2O$	296.8	15366	10189	6.038	4.917	6.065 (+0.45%)	4.915 (−0.04%)	1100	0.8	
	182.5	29014	14670	6.506	4.626	6.488 (−0.28%)	4.599 (−0.59%)	1000	0.7	−100
	84.8	76852	21137	7.218	3.785	7.210 (−0.11%)	3.781 (−0.11%)	1100	0.6	
$K_2Fe(SO_4)_2 \cdot 6\,H_2O$	296.8	14735	10553	5.913	5.004	5.919 (+0.10%)	5.114 (+0.20%)	500	0.8	
	185.6	24872	15370	6.075	4.775	6.128 (+0.86%)	4.776 (+0.02%)	500	0.6	−100
	86.3	59275	26837	6.395	4.303	6.425 (+0.47%)	4.280 (−0.54%)	350	0.5	
	296.8					5.855 (−0.99%)	5.005 (+0.02%)	800	0.8	
	185.6					6.060 (−0.25%)	4.746 (−0.61%)	800	0.6	− 80
	86.3					6.489 (+1.45%)	4.324 (+0.49%)	400	0.5(?)	
$FeSiF_6 \cdot 6\,H_2O$	77.3	29200	48900	4.248	5.497	4.253 (+0.12%)	5.493 (−0.07%)	−1200	0.8	
	20.4	45200	202500	2.715	5.747	2.697 (−0.67%)	5.746 (−0.02%)	−1000	0.8	
	14.2	46300	279600	2.293	5.634	2.283 (−0.44%)	5.659 (+0.44%)	− 950	0.7	
	4.2	17100	588000	0.758	4.443	0.731 (−3.69%)	4.453 (+0.22%)	−1000	1.0	−100
	3.14	9200	614500	0.480	3.932	0.438 (−9.60%)	3.926 (−0.15%)	−1000	0.5	
	1.57	4000	662000	0.220	2.880	0.089 (−147%)	2.883 (+0.10%)	− 950	0.9	
	77.3					4.255 (+0.16%)	5.500 (+0.05%)	− 760	0.7	
	20.4					2.699 (−0.59%)	5.768 (+0.36%)	− 600	0.7	
	14.2					2.289 (−0.17%)	5.627 (−0.12%)	− 600	0.6	
	4.2					0.760 (+0.26%)	4.437 (−0.14%)	− 560	0.9	− 80
	3.14					0.468 (−2.56%)	3.926 (−0.15%)	− 600	0.7	
	1.57					0.138 (−59.4%)	2.897 (+0.59%)	− 560	0.9	

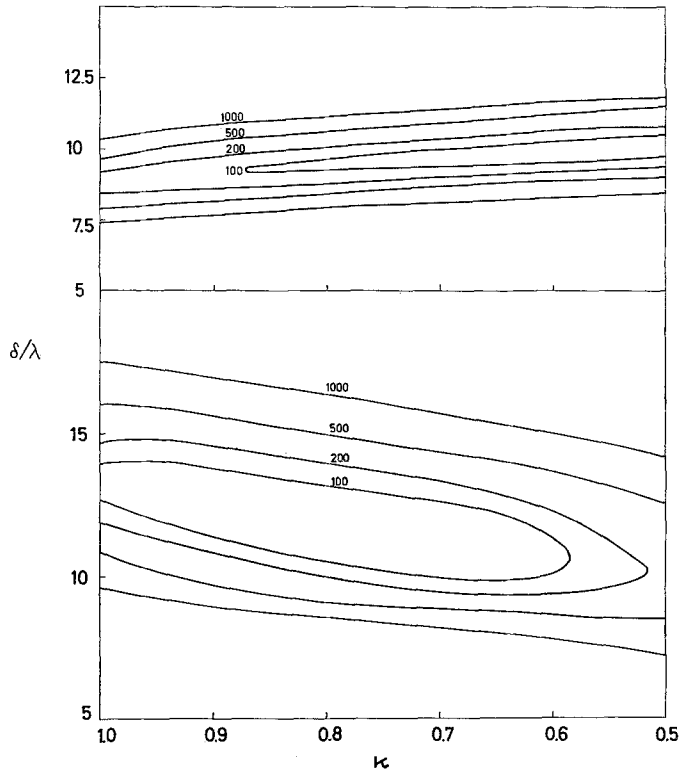

Fig. 7. Curves of constant $\Sigma\Delta^2$ for $FeSiF_6 \cdot 6\,H_2O$, assuming $\lambda = -100$ cm^{-1}. Upper curves for 3.14 °K, lower curves for 77.3 °K. Values of $\Sigma\Delta^2 \times 10^4$ are indicated on the curves

decreasing temperatures. If, on the other hand, smaller absolute values of λ are implied, e.g. $\lambda = -90$ or -80 cm^{-1}, much more negative values of δ/λ are required and, with lowering of temperature, the minimum is displaced to even larger absolute δ/λ (taking $\lambda = -80$ cm^{-1} at $T = 296.8$ °K: $\delta/\lambda = -20, \varkappa = 0.9$; at 182.5 °K: $\delta/\lambda < -30, \varkappa = 0.8$; at 84.8 °K: $\delta/\lambda < -30, \varkappa \sim 0.65$). In this case, the condition $\delta \ll 10$ Dq is not obeyed and the resulting values are thus beyond the range of applicability of the present theory.

A more complicated situation is encountered in the potassium Tutton salt, $K_2Fe(SO_4)_2 \cdot 6\,H_2O$. At temperatures of 296.8 and 185.6 °K, constant values of δ/λ result and, with lowering of temperature, decreasing values of $\varkappa$ are obtained. However, at the lowest temperature investigated, i.e. 86.3 °K, the absolute value of δ/λ is considerably diminished and, in addition, $\varkappa \leqq 0.5$ is found. Practically the same conditions occur for all the values of λ between -100 and -80 cm^{-1}. Thus a "best" fit cannot be obtained. No explanation is offered for the divergence, since additional experimental results will be required to decide which one of the possible reasons applies.

For the iron(II) Tutton salts, $Me_2Fe(SO_4)_2 \cdot 6\,H_2O$, where Me = Rb, Cs, Tl, and for $Tl_2Fe(SeO_4)_2 \cdot 6\,H_2O$, only magnetic anisotropies at room temperature were reported [19]. Although, according to (21), these values determine $K_\parallel - K_\perp$, this information is not sufficient for a reliable theoretical analysis of the data.

In $FeSO_4 \cdot 7\ H_2O$, the Fe^{2+} ion is octahedrally surrounded by six H_2O ligands. Principal molar susceptibilities are available [22], however, no theoretical evaluation of the data is possible, since the unit cell contains eight molecules [26] and their mutual orientation is presently unknown.

In rhombohedral $FeSiF_6 \cdot 6\ H_2O$, there is one molecule per unit cell [7], the ferrous ion being surrounded by a presumably distorted octahedron of water molecules. Here, of course, $\chi_\parallel = K_\parallel$ and $\chi_\perp = K_\perp$. Principal susceptibilities are available at and below 77.3 °K only. At 77.3 °K, a larger value of δ/λ is obtained than the almost constant value which is found at the various lower temperatures investigated. The value of $\varkappa$ is practically constant at the higher temperatures (77.3, 20.4, and 14.2 °K) and amounts to $\sim$0.8 if $\lambda = -100$ cm^{-1} and to $\sim$0.7 if $\lambda = -80$ cm^{-1} is considered. However, at the lowest temperatures (4.2, 3.14, and 1.57 °K), the results are rather insensitive to changes in this parameter, since valleys extending parallel to the $\varkappa$ axis are obtained on the $\sum \Delta^2$ surface (cf. Fig. 7). Thus the values of $\varkappa$ are scattered between 1.0 and 0.5. Also, the results are not extremely sensitive with respect to λ. We list therefore in the Table fits achieved with both $\lambda = -100$ and $\lambda = -80$ cm^{-1}, these being considered as the limits of reasonable λ values. However, the lower total percentage deviation resulting on the assumption of $\lambda = -80$ cm^{-1} indicates that the smaller absolute value of λ is more likely to be correct. Irrespective of the accurate magnitude of the parameters involved, our results confirm the assumption of a trigonally distorted octahedral symmetry [24].

No investigations of the magnetic anisotropy of high-spin cobalt(III) compounds have been reported so far.

Discussion

The present treatment of the magnetic anisotropy and susceptibility of high-spin d^6 systems considers the population of all the levels resulting from a cubic $^5T_2$ ground term. This may be considered as a good approximation, since it is well known that the next cubic term ^5E is $\sim$10,000 cm^{-1} higher in energy*. In addition, the $^5T_2$ is split by a superimposed tetragonal field according to $^5T_2 \rightarrow {}^5B_2 + {}^5E$, whereas $^5E \rightarrow {}^5A_1 + {}^5B_1$. Thus no interconnecting matrix elements occur on application of a tetragonal distortion. This is in general not true, if a trigonal distortion becomes effective, since the splitting is according to $^5T_2 \rightarrow {}^5A_1 + {}^5E$, whereas the upper ^5E is not split. Spin-orbit interaction mixes these low-symmetry states. However, since spin-orbit coupling is rather small ($\lambda = -103$ cm^{-1} for the free iron(II) ion [30], and usually even smaller in a complex), this mixing in of states from the cubic ^5E is completely negligible as far as the magnetic susceptibility is concerned.

It is interesting to realize that although $K_\parallel$ contains both a "low-field" and a "high-field" term, $K_\perp$ contains only the latter. This is caused by the fact that all the diagonal matrix elements of $\mu_\perp$ are zero and is reflected in the value of $g_\perp = 0$. The equality of $P_\parallel$ and $P_\perp$ in the limiting case of octahedral symmetry [31, 32]

* For all high-spin octahedral d^6 complexes studied spectroscopically, triplet states were found to be considerably higher in energy than the ^5E term and can thus be disregarded *a fortiori* [27]. This does not apply to iron(II) compounds having a planar geometry, where triplet ground states were suggested to account for their peculiar magnetic properties [28, 29]. More recently, triplet ground states were found also in certain iron(II)-bis(α-diimine) complexes (cf. part II of the present paper).

is achieved by the additional degeneracy of the magnetically unperturbed levels, since these contribute now to the "low-field" term.

The principal characteristics of the theoretical results, underscored in Fig. 2 to 5, are that, although ligand fields of low symmetry have a comparatively small effect on the average moment [33], unless they lift the orbital degeneracy of the $^5T_2$ term by more than about the magnitude of λ, their influence does show up in the principal moments $P_\parallel$ and $P_\perp$. For larger fields and at low temperatures, the changes as compared to the cubic ligand field are considerable. However, for higher temperatures and for smaller values of $\varkappa$, the moments approach the averaged spin-only value of 4.90 B.M.

The agreement between the calculated principal magnetic moments and the experimental results taken from the literature is in general very good. Most of the experimental data were reproduced by our fitting procedure to better than ~1%. However, the accuracy of the experimental values is in general much lower. This relation should be borne in mind if parameter values determined from such fit are considered.

In $(NH_4)_2Fe(SO_4)_2 \cdot 6\,H_2O$, the only reasonable fit to the available principal moments is achieved using an average value of $\delta = 1070\ cm^{-1}$, $\lambda = -100\ cm^{-1}$ and $\varkappa$ decreasing from 0.8 at 296.8 °K to 0.6 at 84.8 °K. This result is in contrast to the conclusions of Bose et al. [1], which, however, were based on erroneous calculations. The decrease in covalency with increasing temperature seems to be due to the thermal expansion of the crystal lattice and a simultaneous decrease in the overlap between the iron(II) 3*d*- and ligand water charge clouds. The validity of the present approximation is limited mainly by the assumption of strict axial symmetry. Since the presence of a doubly degenerate ground state is implied by $\delta > 0$, deviations from the obtained results are expected whenever this degeneracy is lifted by rhombic or lower field components. Measurements of principal susceptibilities at liquid hydrogen temperature [34] indicate that the splitting of the lowest doublet is small in comparison with kT. Both component levels may therefore be considered approximately degenerate, at least down to 10 °K [34]. Below 2 °K, the lowest doublet is split by ~6.4 cm^{-1} [34—37]. These facts, however, do not invalidate the interpretation given at higher temperatures. From the quadrupole splitting of Mössbauer spectra [38], values of δ considerably smaller than those obtained from susceptibility measurements were reported. No explanation is provided for this difference at present.

In $K_2Fe(SO_4)_2 \cdot 6\,H_2O$, the experimental moment values for the upper two temperatures are well reproduced by the theory, particularly if $\lambda = -100\ cm^{-1}$ is assumed. This has as a consequence $\delta = 500\ cm^{-1}$ and $\varkappa$ decreasing from 0.8 at 296.8 °K to 0.6 at 185.6 °K. The difficulty encountered at 86.3 °K may be due simply to inaccuracy of the experimental data, although different explanations cannot be ruled out at this stage of our knowledge.

In $FeSiF_6 \cdot 6\,H_2O$, the observed principal magnetic moments may be extremely well fitted, particularly if $\lambda = -80\ cm^{-1}$ is used. This is of some importance, since the data on the compound are considered as the most accurate data available on iron(II). The fit at the upper four temperatures (77.3 to 4.2 °K) is good to at least 0.6%. The value of $\delta = -760\ cm^{-1}$ at 77.3 °K is identical with the value resulting from Mössbauer spectroscopy [38] and in very good agreement with the

analysis of susceptibility data performed by EICHER [3], who arrived at $\delta = -730$ cm^{-1}. It seems reasonable to average the scattered parameter values at temperatures between 20.4 and 1.57 °K, yielding $\delta \sim -580$ cm^{-1} and $\varkappa \sim 0.8$ or 0.7. The only exception to the good fit are the values of $P_\parallel$ at the lowest two temperatures, especially at 1.57 °K. JACKSON [24] mentions that this experimental value is not precise due to a cross susceptibility correction which assumes ~40%. It should be remarked that PRYCE [23, 24] and PALUMBO [39] could approximate this value to only 25%. The comparatively good fit to the data, which is obtained with $\lambda = -100$ cm^{-1}, makes clear how PALUMBO [39] arrived at his results characterized by $\delta = -1200$ cm^{-1}. Finally, a recent analysis of powder susceptibilities [40], which arrived at $\delta = -135$ cm^{-1}, demonstrates that the less rigorous but often employed approach of comparing calculated and experimental μ_{eff} curves may not always yield useful results.

In comparison to other ions of the iron group, information about ground state splittings in iron(II) from paramagnetic resonance data is completely lacking. Only weak lines were reported in potassium and ammonium Tutton salts [41, 42] as well as in iron(II) fluosilicate hexahydrate [42], all at 20 °K. Since, in axial symmetry, the corresponding transitions are rigorously forbidden, paramagnetic resonance investigations on iron(II) compounds where a high microsymmetry is expected do not look very promising. The only definite resonance data analyzed in detail are those of iron(II) substitutionally present in MgO [43] and in ZnF_2 [11, 44], where the finite line intensity is due to low symmetry distortions in the crystal.

It is partly for this reason that more accurate and detailed experimental data on principal magnetic susceptibilities of the compounds discussed above, and possibly other high-spin iron(II) complex salts should be collected.

Conclusions

The present investigation demonstrates for the d^6 electron configuration that in some compounds, unique sets of values for the molecular parameters λ, δ, $\varkappa$, and alike may be arrived at by a rigorous theoretical analysis of single crystal magnetic susceptibility data. In other compounds, however, no unique fit is possible and additional results, possibly from different physical measurements, are required to enable a selection of the reasonable parameter values. Previous results of theoretical analyses of magnetic susceptibility data, which were based on less complete computations, have to be reconsidered. It is likely that these conclusions may be extended to other d^n configurations as well.

Acknowledgements. The authors appreciate the hospitality of Mellon Institute, where the larger part of this investigation was carried out. Thanks are due to Dr. N. URYU for several suggestions, to Dr. J. R. PERUMAREDDI for help in checking the algebra, and to Mr. R. L. ANDERSON for programming of the calculations on the IBM 7090 computer of the University of Pittsburgh.

Appendix I

Energies and Wave-functions of the $^5T_2$ Term under the Action of an Axial Ligand Field and of Spin-orbit Coupling

The matrices of the ligand field and of spin-orbit coupling may be written as

$$
\begin{array}{c} \\ |-1,1\rangle \\ |0,0\rangle \\ |1,-1\rangle \end{array}
\begin{array}{c}
\begin{array}{ccc} |-1,1\rangle & |0,0\rangle & |1,-1\rangle \end{array} \\
\begin{pmatrix} \lambda_\parallel & -\sqrt{3}\lambda_\perp & 0 \\ -\sqrt{3}\lambda_\perp & \Delta & -\sqrt{3}\lambda_\perp \\ 0 & -\sqrt{3}\lambda_\perp & \lambda_\parallel \end{pmatrix}
\end{array}
\quad (M_J = 0)\,,
$$

$$
\begin{array}{c} \\ |1,0\rangle \\ |0,1\rangle \\ |-1,2\rangle \end{array}
\begin{array}{c}
\begin{array}{ccc} |1,0\rangle & |0,1\rangle & |-1,2\rangle \end{array} \\
\begin{pmatrix} 0 & -\sqrt{3}\lambda_\perp & 0 \\ -\sqrt{3}\lambda_\perp & \Delta & -\sqrt{2}\lambda_\perp \\ 0 & -\sqrt{2}\lambda_\perp & 2\lambda_\parallel \end{pmatrix}
\end{array}
\quad (M_J = \pm 1), \qquad \text{(I-1)}
$$

$$
\begin{array}{c} \\ |0,2\rangle \\ |1,1\rangle \end{array}
\begin{array}{c}
\begin{array}{cc} |0,2\rangle & |1,1\rangle \end{array} \\
\begin{pmatrix} \Delta & -\sqrt{2}\lambda_\perp \\ -\sqrt{2}\lambda_\perp & -\lambda_\parallel \end{pmatrix}
\end{array}
\quad (M_J = \pm 2)\,,
$$

$$
\begin{array}{c} \\ |1,2\rangle \end{array}
\begin{array}{c}
\begin{array}{c} |1,2\rangle \end{array} \\
\begin{pmatrix} -2\lambda_\parallel \end{pmatrix}
\end{array}
\quad (M_J = \pm 3)\,.
$$

The first matrix ($M_J = 0$) may be factorized further and gives the energies

$$
\begin{aligned}
E_0 &= \tfrac{1}{2}\left[(\lambda_\parallel + \Delta) - \{(\lambda_\parallel - \Delta)^2 + 24\,\lambda_\perp^2\}^{1/2}\right] \\
E_0' &= \tfrac{1}{2}\left[(\lambda_\parallel + \Delta) + \{(\lambda_\parallel - \Delta)^2 + 24\,\lambda_\perp^2\}^{1/2}\right] \\
E_0'' &= \lambda_\parallel\,.
\end{aligned} \qquad \text{(I-2)}
$$

The energies for $M_J = \pm 1$ are determined by the roots of the cubic

$$
x^3 - (2 + \eta)\,x^2 + (2\,\eta - 5\,\varepsilon^2)\,x + 6\,\varepsilon^2 = 0\,, \qquad \text{(I-3)}
$$

where $x = E_i/\lambda_\parallel$, E_i being E_1, E_1'', and E_1' respectively, $\eta = \delta/\lambda_\parallel$ and $\varepsilon = \lambda_\perp/\lambda_\parallel$. The energies are labeled such that E_1 becomes the lowest one, followed by E_1'' and E_1' (cf. Fig. 1),

$$
E_1 < E_1'' < E_1'\,. \qquad \text{(I-4)}
$$

The remaining energies are given by

$$
\begin{aligned}
E_2 &= \tfrac{1}{2}\left[(\Delta - \lambda_\parallel) - \{(\Delta + \lambda_\parallel)^2 + 8\,\lambda_\perp^2\}^{1/2}\right] \\
E_2' &= \tfrac{1}{2}\left[(\Delta - \lambda_\parallel) + \{(\Delta + \lambda_\parallel)^2 + 8\,\lambda_\perp^2\}^{1/2}\right] \\
E_3 &= -2\,\lambda_\parallel\,.
\end{aligned} \qquad \text{(I-5)}
$$

The corresponding wave-functions may be written as

$$
\begin{aligned}
\psi_1 &= a_1\,|\,1,0\rangle + b_1\,|\,0,1\rangle + c_1\,|-1,2\rangle \\
\psi_{-1} &= a_1\,|-1,0\rangle + b_1\,|\,0,-1\rangle + c_1\,|\,1,-2\rangle \\
\psi_0 &= a_0\,|\,1,-1\rangle + b_0\,|\,0,0\rangle + a_0\,|-1,1\rangle \\
\psi_0'' &= (1/\sqrt{2})\,|\,1,-1\rangle - (1/\sqrt{2})\,|-1,1\rangle \\
\psi_1'' &= a_1''\,|\,1,0\rangle + b_1''\,|\,0,1\rangle + c_1''\,|-1,2\rangle \\
\psi_{-1}'' &= a_1''\,|-1,0\rangle + b_1''\,|\,0,-1\rangle + c_1''\,|\,1,-2\rangle \\
\psi_2 &= a_2\,|\,0,2\rangle + b_2\,|\,1,1\rangle \\
\psi_{-2} &= a_2\,|\,0,-2\rangle + b_2\,|-1,-1\rangle \\
\psi_3 &= |\,1,2\rangle
\end{aligned} \qquad \text{(I-6)}
$$

$$
\begin{aligned}
\psi_{-3} &= |-1,-2\rangle \\
\psi'_2 &= b_2 \,|\, 0,2\rangle - a_2 \,|\, 1,1\rangle \\
\psi'_{-2} &= b_2 \,|\, 0,-2\rangle - a_2 \,|-1,-1\rangle \\
\psi'_1 &= a'_1 \,|\, 1,0\rangle + b'_1 \,|\, 0,1\rangle + c'_1 \,|-1,2\rangle \\
\psi'_{-1} &= a'_1 \,|-1,0\rangle + b'_1 \,|\, 0,-1\rangle + c'_1 \,|\, 1,-2\rangle \\
\psi'_0 &= (1/\sqrt{2})\, b_0 \,|\, 1,-1\rangle - \sqrt{2}\, a_0 \,|\, 0,0\rangle + (1/\sqrt{2})\, b_0 \,|-1,1\rangle ,
\end{aligned}
\tag{I-6}
$$

where the coefficients a_1, b_1, c_1 etc. are obtained from the set of linear equations corresponding to (I-1) and the normalization condition and are given by

$$
\begin{aligned}
a_1 &= -\frac{\sqrt{3}(2\lambda_\parallel - E_1)}{\sqrt{2}\, E_1}\, c_1 , \\
b_1 &= \frac{(2\lambda_\parallel - E_1)}{\sqrt{2}\, \lambda_\perp}\, c_1 , \\
c_1 &= \left[\frac{3\,(2\lambda_\parallel - E_1)^2}{2\, E_1^2} + \frac{(2\lambda_\parallel - E_1)^2}{2\,\lambda_\perp^2} + 1\right]^{-1/2} .
\end{aligned}
\tag{I-7}
$$

The coefficients a'_1, b'_1, and c'_1 are obtained from (I-7) by replacing E_1 by E'_1 and, similarly, a''_1, b''_1, and c''_1 are obtained by replacing E_1 by E''_1. Also,

$$
\begin{aligned}
a_0 &= \frac{\sqrt{3}\,\lambda_\perp}{(\lambda_\parallel - E_0)}\, b_0 \\
b_0 &= \left[\frac{6\,\lambda_\perp^2}{(\lambda_\parallel - E_0)^2} + 1\right]^{-1/2}
\end{aligned}
\tag{I-8}
$$

and

$$
\begin{aligned}
a_2 &= \frac{\sqrt{2}\,\lambda_\perp}{(\Delta - E_2)}\, b_2 , \\
b_2 &= \left[\frac{2\,\lambda_\perp^2}{(\Delta - E_2)^2} + 1\right]^{-1/2} .
\end{aligned}
\tag{I-9}
$$

Appendix II

Matrix Elements of the Magnetic Operators $\mu_\parallel$ and $\mu_\perp$

$$
\begin{aligned}
G_{1z}^{E_1} &= 2\,\{\langle\psi_1 \,|\, \mu_\parallel \,|\, \psi_1\rangle\}^2 = 2\,\{(4+\varkappa_\parallel)\, c_1^2 + 2\, b_1^2 - \varkappa_\parallel\, a_{1j}^2\}^2 \\
G_{1z}^{E''_1} &= 2\,\{\langle\psi''_1 \,|\, \mu_\parallel \,|\, \psi''_1\rangle\}^2 = 2\,\{(4+\varkappa_\parallel)\, c_1''^2 + 2\, b_1''^2 - \varkappa_\parallel\, a_1''^2\}^2 \\
G_{1z}^{E_2} &= 2\,\{\langle\psi_2 \,|\, \mu_\parallel \,|\, \psi_2\rangle\}^2 = 2\,\{4\, a_2^2 + (2-\varkappa_\parallel)\, b_2^2\}^2 \\
G_{1z}^{E_3} &= 2\,\{\langle\psi_3 \,|\, \mu_\parallel \,|\, \psi_3\rangle\}^2 = 2\,(4-\varkappa_\parallel)^2 \\
G_{1z}^{E'_2} &= 2\,\{\langle\psi'_2 \,|\, \mu_\parallel \,|\, \psi'_2\rangle\}^2 = 2\,\{4\, b_2^2 + (2-\varkappa_\parallel)\, a_2^2\}^2 \\
G_{1z}^{E'_1} &= 2\,\{\langle\psi'_1 \,|\, \mu_\parallel \,|\, \psi'_1\rangle\}^2 = 2\,\{(4+\varkappa_\parallel)\, c_1'^2 + 2\, b_1'^2 - \varkappa_\parallel\, a_1'^2\}^2 \\
G_{2z}^{E_1} &= \frac{2\,|\langle\psi_1 \,|\, \mu_\parallel \,|\, \psi''_1\rangle|^2}{E''_1 - E_1} + \frac{2\,|\langle\psi_1 \,|\, \mu_\parallel \,|\, \psi'_1\rangle|^2}{E'_1 - E_1} \\
G_{2z}^{E_0} &= \frac{2\,|\langle\psi_0 \,|\, \mu_\parallel \,|\, \psi''_0\rangle|^2}{E''_0 - E_0} \\
G_{2z}^{E''_0} &= -\frac{2\,|\langle\psi''_0 \,|\, \mu_\parallel \,|\, \psi_0\rangle|^2}{E''_0 - E_0} + \frac{2\,|\langle\psi''_0 \,|\, \mu_\parallel \,|\, \psi'_0\rangle|^2}{E'_0 - E''_0} \\
G_{2z}^{E''_1} &= -\frac{2\,|\langle\psi''_1 \,|\, \mu_\parallel \,|\, \psi_1\rangle|^2}{E''_1 - E_1} - \frac{2\,|\langle\psi''_1 \,|\, \mu_\parallel \,|\, \psi'_1\rangle|^2}{E'_1 - E''_1}
\end{aligned}
\tag{II-1}
$$

$$
\begin{aligned}
G_{2z}^{E_2} &= \frac{2\,|\langle\psi_2 \mid \mu_\parallel \mid \psi_2'\rangle|^2}{E_2' - E_2} \\
G_{2z}^{E_2'} &= -\frac{2\,|\langle\psi_2' \mid \mu_\parallel \mid \psi_2\rangle|^2}{E_2' - E_2} \\
G_{2z}^{E_1'} &= -\frac{2\,|\langle\psi_1' \mid \mu_\parallel \mid \psi_1\rangle|^2}{E_1' - E_1} - \frac{2\,|\langle\psi_1' \mid \mu_\parallel \mid \psi_1''\rangle|^2}{E_1' - E_1''} \\
G_{2z}^{E_0'} &= -\frac{2\,|\langle\psi_0' \mid \mu_\parallel \mid \psi_0''\rangle|^2}{E_0' - E_0''}
\end{aligned}
\tag{II-1}
$$

$$
\begin{aligned}
\langle\psi_1 \mid \mu_\parallel \mid \psi_1''\rangle &= (4 + \varkappa_\parallel)\, c_1 c_1'' + 2\, b_1 b_1'' - \varkappa_\parallel\, a_1 a_1'' \\
\langle\psi_1 \mid \mu_\parallel \mid \psi_1'\rangle &= (4 + \varkappa_\parallel)\, c_1 c_1' + 2\, b_1 b_1' - \varkappa_\parallel\, a_1 a_1' \\
\langle\psi_0 \mid \mu_\parallel \mid \psi_0''\rangle &= -\sqrt{2}\,(2 + \varkappa_\parallel)\, a_0 \\
\langle\psi_0' \mid \mu_\parallel \mid \psi_0''\rangle &= -(2 + \varkappa_\parallel)\, b_0 \\
\langle\psi_1' \mid \mu_\parallel \mid \psi_1''\rangle &= (4 + \varkappa_\parallel)\, c_1'' c_1' + 2\, b_1'' b_1' - \varkappa_\parallel\, a_1'' a_1' \\
\langle\psi_2 \mid \mu_\parallel \mid \psi_2'\rangle &= (2 + \varkappa_\parallel)\, a_2 b_2
\end{aligned}
\tag{II-2}
$$

$$
\begin{aligned}
G_{2x}^{E_1} &= \frac{2A^2}{E_0 - E_1} + \frac{2A_1^2}{E_0'' - E_1} + \frac{2A_2^2}{E_2 - E_1} + \frac{2A_3^2}{E_2' - E_1} + \frac{2A_{14}^2}{E_0' - E_1} \\
G_{2x}^{E_0} &= -\frac{2A^2}{E_0 - E_1} + \frac{2A_4^2}{E_1'' - E_0} + \frac{2A_5^2}{E_1' - E_0} \\
G_{2x}^{E_0''} &= -\frac{2A_1^2}{E_0'' - E_1} + \frac{2A_6^2}{E_1'' - E_0''} + \frac{2A_7^2}{E_1' - E_0''} \\
G_{2x}^{E_1''} &= -\frac{2A_4^2}{E_1'' - E_0} - \frac{2A_6^2}{E_1'' - E_0''} + \frac{2A_8^2}{E_2 - E_1''} + \frac{2A_9^2}{E_2' - E_1''} + \frac{2A_{15}^2}{E_0' - E_1''} \\
G_{2x}^{E_2} &= -\frac{2A_2^2}{E_2 - E_1} - \frac{2A_8^2}{E_2 - E_1''} + \frac{2A_{10}^2}{E_3 - E_2} + \frac{2A_{11}^2}{E_1' - E_2} \\
G_{2x}^{E_3} &= -\frac{2A_{10}^2}{E_3 - E_2} + \frac{2A_{12}^2}{E_2' - E_3} \\
G_{2x}^{E_2'} &= -\frac{2A_3^2}{E_2' - E_1} - \frac{2A_9^2}{E_2' - E_1''} - \frac{2A_{12}^2}{E_2' - E_3} + \frac{2A_{13}^2}{E_1' - E_2'} \\
G_{2x}^{E_1'} &= -\frac{2A_5^2}{E_1' - E_0} - \frac{2A_7^2}{E_1' - E_0''} - \frac{2A_{11}^2}{E_1' - E_2} - \frac{2A_{13}^2}{E_1' - E_2'} + \frac{2A_{16}^2}{E_0' - E_1'} \\
G_{2x}^{E_0'} &= -\frac{2A_{14}^2}{E_0' - E_1} - \frac{2A_{15}^2}{E_0' - E_1''} - \frac{2A_{16}^2}{E_0' - E_1'}
\end{aligned}
\tag{II-3}
$$

$$
\begin{aligned}
A &= \langle\psi_1 \mid \mu_\perp \mid \psi_0\rangle = \sqrt{6}\, a_1 a_0 - (1/\sqrt{2})\, \varkappa_\perp\, a_1 b_0 + \sqrt{6}\, b_1 b_0 - (1/\sqrt{2})\, \varkappa_\perp\, b_1 a_0 + 2 c_1 a_0 \\
A_1 &= \langle\psi_1 \mid \mu_\perp \mid \psi_0''\rangle = \sqrt{3}\, a_1 + \tfrac{1}{2}\, \varkappa_\perp b_1 - \sqrt{2}\, c_1 \\
A_2 &= \langle\psi_1 \mid \mu_\perp \mid \psi_2\rangle = \sqrt{6}\, a_1 b_2 + 2\, b_1 a_2 - (1/\sqrt{2})\, \varkappa_\perp\, b_1 b_2 - (1/\sqrt{2})\, \varkappa_\perp\, c_1 a_2 \\
A_3 &= \langle\psi_1 \mid \mu_\perp \mid \psi_2'\rangle = -\sqrt{6}\, a_1 a_2 + 2\, b_1 b_2 + (1/\sqrt{2})\, \varkappa_\perp\, b_1 a_2 - (1/\sqrt{2})\, \varkappa_\perp\, c_1 b_2 \\
A_4 &= \langle\psi_1'' \mid \mu_\perp \mid \psi_0\rangle = \sqrt{6}\, a_1'' a_0 - (1/\sqrt{2})\, \varkappa_\perp\, a_1'' b_0 + \sqrt{6}\, b_1'' b_0 - (1/\sqrt{2})\, \varkappa_\perp\, b_1'' a_0 + 2\, c_1'' a_0 \\
A_5 &= \langle\psi_1' \mid \mu_\perp \mid \psi_0\rangle = \sqrt{6}\, a_1' a_0 - (1/\sqrt{2})\, \varkappa_\perp\, a_1' b_0 + \sqrt{6}\, b_1' b_0 - (1/\sqrt{2})\, \varkappa_\perp\, b_1' a_0 + 2\, c_1' a_0 \\
A_6 &= \langle\psi_1'' \mid \mu_\perp \mid \psi_0''\rangle = \sqrt{3}\, a_1'' + \tfrac{1}{2}\, \varkappa_\perp\, b_1'' - \sqrt{2}\, c_1'' \\
A_7 &= \langle\psi_1' \mid \mu_\perp \mid \psi_0''\rangle = \sqrt{3}\, a_1' + \tfrac{1}{2}\, \varkappa_\perp\, b_1' - \sqrt{2}\, c_1'
\end{aligned}
\tag{II-4}
$$

$$
\begin{aligned}
A_8 &= \langle\psi_1''\,|\,\mu_\perp\,|\,\psi_2\rangle = \sqrt{6}\,a_1''b_2 + 2\,b_1''a_2 - (1/\sqrt{2})\,\varkappa_\perp\,b_1''b_2 - (1/\sqrt{2})\,\varkappa_\perp\,c_1''a_2\\
A_9 &= \langle\psi_1''\,|\,\mu_\perp\,|\,\psi_2'\rangle = -\sqrt{6}\,a_1''a_2 + 2\,b_1''b_2 + (1/\sqrt{2})\,\varkappa_\perp\,b_1''a_2 - (1/\sqrt{2})\,\varkappa_\perp\,c_1''b_2\\
A_{10} &= \langle\psi_2\,|\,\mu_\perp\,|\,\psi_3\rangle = -(1/\sqrt{2})\,\varkappa_\perp\,a_2 + 2\,b_2\\
A_{11} &= \langle\psi_1'\,|\,\mu_\perp\,|\,\psi_2\rangle = \sqrt{6}\,a_1'b_2 + 2\,b_1'a_2 - (1/\sqrt{2})\,\varkappa_\perp\,b_1'b_2 - (1/\sqrt{2})\,\varkappa_\perp\,c_1'a_2\\
A_{12} &= \langle\psi_2'\,|\,\mu_\perp\,|\,\psi_3\rangle = -(1/\sqrt{2})\,\varkappa_\perp\,b_2 - 2\,a_2 \qquad \text{(II-4)}\\
A_{13} &= \langle\psi_1'\,|\,\mu_\perp\,|\,\psi_2'\rangle = -\sqrt{6}\,a_1'a_2 + 2\,b_1'b_2 + (1/\sqrt{2})\,\varkappa_\perp\,b_1'a_2 - (1/\sqrt{2})\,\varkappa_\perp\,c_1'b_2\\
A_{14} &= \langle\psi_0'\,|\,\mu_\perp\,|\,\psi_1\rangle = \sqrt{3}\,b_0a_1 + \varkappa_\perp\,a_1a_0 - 2\sqrt{3}\,a_0b_1 - \tfrac{1}{2}\,\varkappa_\perp\,b_0b_1 + \sqrt{2}\,b_0c_1\\
A_{15} &= \langle\psi_0'\,|\,\mu_\perp\,|\,\psi_1''\rangle = \sqrt{3}\,b_0a_1'' + \varkappa_\perp\,a_1''a_0 - 2\sqrt{3}\,a_0b_1'' - \tfrac{1}{2}\,\varkappa_\perp\,b_0b_1'' + \sqrt{2}\,b_0c_1''\\
A_{16} &= \langle\psi_0'\,|\,\mu_\perp\,|\,\psi_1'\rangle = \sqrt{3}\,b_0a_1' + \varkappa_\perp\,a_1'a_0 - 2\sqrt{3}\,a_0b_1' - \tfrac{1}{2}\,\varkappa_\perp\,b_0b_1' + \sqrt{2}\,b_0c_1'\,.
\end{aligned}
$$

References

1. Bose, A., A. S. Chakravarty, and R. Chatterjee: Proc. Roy. Soc. (London) **A 261**, 207 (1961).
2. Palumbo, D.: Nuovo Cimento [10] 8, 271 (1958).
3. Eicher, H.: Z. Physik **171**, 582 (1963).
4. Stout, J. W., and S. A. Reed: J. Am. chem. Soc. **76**, 5279 (1954).
5. Wyckoff, R. W. G.: Crystal structures, Vol. 1, second edition. New York: Interscience Publishers.
6. Hofmann, W.: Z. Krist. **78**, 279 (1931).
7. Hassel, O., and J. R. Salvesen: Z. physik. Chem. **128**, 345 (1927).
8. Cotton, F. A., and G. Wilkinson: Advanced inorganic chemistry. New York: Interscience Publishers 1962.
9. Figgis, B. N.: Trans. Faraday Soc. **57**, 198 (1961).
10. Gladney, H. M., and J. D. Swalen: J. chem. Physics **42**, 1999 (1965).
11. Tinkham, M.: Proc. Roy. Soc. (London) **A 236**, 549 (1956).
12. Low, W.: Paramagnetic resonance in solids. Solid state physics, Suppl. **2**. New York: Academic Press 1960.
13. Stevens, K. W. H.: Proc. Roy. Soc. (London) **A 219**, 542 (1953).
14. Abragam, A., and M. H. L. Pryce: Proc. Roy. Soc. (London) **A 205**, 135 (1951).
15. Van Vleck, J. H.: The theory of electric and magnetic susceptibilities. Oxford: University Press 1932.
16. Bose, A., A. S. Chakravarty, and R. Chatterjee: Proc. Roy. Soc. (London) **A 255**, 145 (1960).
17. Finke, W.: Ann. Physik **31**, 149 (1910).
18. Krishnan, K. S., N. C. Chakravorty, and S. Banerjee: Phil. Trans. Roy. Soc. (London) **A 232**, 99 (1934).
19. —, and A. Mookherji: Phil. Trans. Roy. Soc. (London) **A 237**, 135 (1939).
20. Datta, S.: Ind. J. Physics **28**, 239 (1954).
21. Bose, A.: Ind. J. Physics **22**, 483 (1948).
22. Guha, B. C.: Proc. Roy. Soc. (London) **A 206**, 353 (1951).
23. Pryce, M. H. L.: Nuovo Cimento [10] **6**, Suppl. No. 3, 817 (1957).
24. Jackson, L. C.: Phil. Mag. [8] **4**, 269 (1959).
25. — Phil. Trans. Roy. Soc. (London) **A 224**, 1 (1924).
26. Ness, I.: Naturwiss. **28**, 78 (1940).
27. Jørgensen, C. K.: Absorption spectra and chemical bonding in complexes. London: Pergamon Press 1962.
28. Lever, A. B. P.: J. chem. Soc. **1965**, 1821.
29. Chatt, J., and B. L. Shaw: J. chem. Soc. **1961**, 285.
30. Griffith, J. S.: The theory of transition metal ions. Cambridge: University Press 1961.
31. — Trans. Faraday Soc. **54**, 1109 (1958).
32. Figgis, B. N.: Nature **182**, 1568 (1958).
33. König, E., A. S. Chakravarty, and K. Madeja: Theoret. chim. Acta **9**, 171 (1967).
34. Ohtsuka, T., H. Abe, and E. Kanda: Sci. Rept. Res. Inst. Tohoku Univ. **A9**, 476 (1957).

35. RICHARDSON, J. T., and R. C. SAPP: J. chem. Physics **29**, 337 (1958).
36. SAPP, R. C.: J. chem. Physics **30**, 326 (1959).
37. HILL, R. W., and P. L. SMITH: Proc. physic. Soc. (London) **A 66**, 228 (1953).
38. INGALLS, R.: Physic. Rev. **133**, A787 (1964).
39. PALUMBO, D.: Nuovo Cimento [10] 8, 271 (1958).
40. FIGGIS, B. N., J. LEWIS, F. MABBS, and G. A. WEBB: Nature **203**, 1138 (1964).
41. BAGGULEY, D. M. S., B. BLEANEY, J. H. E. GRIFFITHS, R. P. PENROSE, and B. I. PLUMPTON: Proc. physic. Soc. (London) **61**, 551 (1948).
42. BAKER, J. M., and B. BLEANEY, in BLEANEY, B., and K. W. H. STEVENS, Rept. Progr. Physics **16**, 108 (1953).
43. LOW, W.: Ann. New York Acad. Sci. **72**, 69 (1958); Physic. Rev. **101**, 1827 (1956).
44. TINKHAM, M.: Proc. Roy. Soc. (London) **A 236**, 535 (1956).

Dr. E. KÖNIG
Institut für physikalische Chemie II
der Universität Erlangen-Nürnberg
8520 Erlangen, Fahrstraße 17